IJE TRANSACTIONS C: Aspects Vol. 28, No. 6, (June 2015) 956-963

International Journal of Engineering

Journal Homepage: www.ije.ir

Numerical Simulation of Cavitation in Mixed Flow Pump

Y. Vazifeshenas, M. Farhadi*, K. Sedighi , R. Shafaghat

Faculty of Mechanical Engineering, Babol University of Technology, Babol, Iran

PAPER INFO

Paper history:
Received 23 April 2014
Received in revised form 05 June 2015
Accepted 11 June 2015

Keywords:
Mixed-flow Pump
Multiple Reference Frame
Computational Fluid Dynamics
Cavitation

ABSTRACT

The purpose of this study is to investigate the performance and three-dimensional behavior of the flow in a mixed flow pump and the way cavitation phenomenon is affected by different parameters such as fluid temperature, pump speed and flow rate. Computational fluid dynamic software FLUENT was utilized to simulate the whole flow field of the pump. RNG k-ε model combined with standard wall functions was chosen to deal with the turbulent feature of the problem. The studied pump had four blades mounted on a conical hub which formed the rotary part and nine static vanes afterward as the stationary part. So the rotor-stator interaction was treated with a Multiple Reference Frame (MRF) technique. The flow rates and pump speed were the key parameters for investigation. While the flow rates variation and the pump revolution changed cavitation occurrence widely, the temperature variations caused by weather changes during a year had little effect on cavitation. The cavitation region which is defined by the saturation pressure in that temperature was shown for various cases on a blade.

doi: *10.5829/idosi.ije.2015.28.06c.17*

1. INTRODUCTION

The mixed-flow pump is widely applied in hydraulic engineering applications, so the study on the mixed-flow pump became a hot research topic for many researchers. In a mixed-flow pump, the flow is remarkably influenced by parameters like turbulence and viscosity. The tip clearance can lead to the tip vortexes and non-uniform flow. Nowadays, applying numerical tools to design and optimize the hydraulics of pumps is a standard approach in the industry. Numerical simulation and mathematical treatment have long been used as powerful tools for investigating the complex flow phenomena that occur in the pump system workspace. The physical phenomena involved in complex flow field take a lot of studies to understand [1]. Alpan [2] analyzed an axial flow pump experimentally and focused on the suction reverse flow. Zierke [3, 4] presented an experimental technology and reviewed the flow behavior of high Reynolds number pumps and the flow at the tip clearance. Dupont et al. [5] investigated the rotor-stator interactions in a vaned-diffuser radial-flow pump and unsteady effects in that special case. Li [6] and Wang [7, 8] verified the performance of an axial-flow pump considering the effect of an inducer on it, and also simulated a large-bore axial-flow pump with half-elbow suction sump by a steady numerical approach, and focused on the pressure fluctuation of unsteady flow in the axial-flow pump. In recent years, many researchers simulated and analyzed the flow field in the axial-flow pump [9-14].

In an overall standpoint, in hydraulic systems, fluid mixtures can be categorized into five states according to the operating conditions: (1) fully degassed liquid; (2) fully degassed liquid with vapor; (3) liquid with dissolved gas; (4) liquid with dissolved and undissolved gas and (5) liquid with dissolved gas, undissolved gas and vapor.

Cavitation denotes the process of vaporization, formation and collapse of vapor bubbles in regions of a flowing liquid, where the pressure falls below its vapor pressure and increases subsequently. Cavitation is an undesirable occurrence in many existing cases. In fact cavitation puts negative effect on devices such as propellers and pumps, make a noise, damage to components, vibrations, and a loss of efficiency. Hence

*Corresponding Author's Email: mfarhadi@nit.ac.ir (M. Farhadi)

Please cite this article as: Y. Vazifeshenas, M. Farhadi, K. Sedighi , R. Shafaghat, Numerical Simulation of Cavitation in Mixed Flow Pump, International Journal of Engineering (IJE), TRANSACTIONS C: Aspects Vol. 28, No. 6, (June 2015) 956-963

cavitating flows investigations are of interest in many scientific and technical problems.

For modeling purposes in engineering, it is assumed that the local pressures are equal to the vapor pressure when vaporous cavitation is taking place [15].

In order to detect the beginning of cavitation and its development, there are different engineering techniques. Amongst them, following items are frequently utilized: (1) considering the net positive suction head (NPSH) and the drop in the total delivery head at a constant flow rate, (2) visualization of the flow through a transparent impeller eye, (3) paint erosion test, which is based on painting the impeller blades and observing the cavitation erosion by evident removal of the paint, (4) measurement of the static pressure within the flow field, (5) measurement of the vibration of the structure and its belongings, by mounting a transducer in the pump inlet near the impeller blades or as close as possible to the place of implosion of bubbles, (6) measurement of the ultrasound by acoustic emission sensor which defines special frequencies, and (7) measurement of sound pressure in audible range [16].

Definitely, static pressure governs the process of vapor bubble formation or boiling [17]. In most cases, cavitation can occur near the fast moving blades of the turbine where the local dynamic head increases due to the action of blades which reduces the static pressure. Cavitation seldom occurs on the guide vane surface because the static pressure reduction is less in that region.

Model tests are generally used to detect cavitation in a hydraulic turbine [18, 19] and to investigate the cavitation structures [20, 21]. On the other hand, the CFD approach is also widely and successfully used in cavitation studies, and as a useful tool, can give realistic results in cavitation simulations and predictions [22-27].

One of the main important parameters in the large scale industrial pump is cavitation. Numerical simulation is one of the powerful techniques for prediction of cavitation in these devices. In this study, the three-dimensional steady simulation of turbulent flow inside the full passage of a mixed flow pump using CFD commercial software FLUENT 6.3 was conducted to predict cavitation occurrence in Mashad power plant mixed cooling water pump. Results are presented in the form of pressure contour, streamlines and cavitation occurrence area. The effects of flow temperature, pump speed and intake flow rate on cavitation occurrence were analyzed.

2. GOVERNING EQUATIONS

The three-dimensional Reynolds-averaged Navier-Stokes equations for steady incompressible flow encountered in this problem, for the conservation of mass and momentum are given as:

$$\frac{\partial}{\partial x_i}(\rho \bar{u}_i) = 0 \tag{1}$$

$$\frac{\partial}{\partial x_j}(\rho \bar{u}_i \bar{u}_j) = -\frac{\partial \bar{p}}{\partial x_i} + \frac{\partial}{\partial x_j}\left(\mu \frac{\partial \bar{u}_i}{\partial x_j} - \rho \bar{u}_i \bar{u}_j \right) \tag{2}$$

where μ is the molecular viscosity, $\bar{p}$ is the averaged pressure and $-\rho \bar{u}_i \bar{u}_j$ represents the Reynolds stress. To achieve the closure of Equation (2) the Reynolds stresses are modeled. The Reynolds stresses are given by:

$$-\rho \bar{u}_i \bar{u}_j = \mu_t \left(\frac{\partial \bar{u}_i}{\partial x_j} + \frac{\partial \bar{u}_j}{\partial x_i} \right) - \frac{2}{3}\delta_{ij} \cdot \left(\rho k + \mu_t \frac{\partial \bar{u}_i}{\partial x_i} \right) \tag{3}$$

where k is the turbulent kinetic energy and μ_t is the turbulent viscosity.

In order to compute the turbulent viscosity for turbulence model such as k-ε variants, two additional transport equations for the turbulence kinetic energy, k, and turbulence dissipation rate, ε, must be solved.

2. 1. RNG k- ε Model The RNG k-ε model was derived using a rigorous statistical technique (called renormalization group theory). Turbulence, in general, is affected by rotation or swirl in the mean flow. The effect of swirl on turbulence is included in the RNG model, enhancing accuracy for swirling flows. Comprehensive description of RNG model and its usages in turbulence model can be found in literature [28]. The following transport equations give the turbulence kinetic energy, k, and turbulence dissipation rate, ε:

$$\frac{\partial (\rho k \bar{u}_i)}{\partial x_i} = \frac{\partial}{\partial x_j}\left(\alpha_k \mu_{eff} \frac{\partial k}{\partial x_j} \right) + G_k - \rho \varepsilon \tag{4}$$

$$\frac{\partial (\rho \varepsilon \bar{u}_i)}{\partial x_i} = \frac{\partial}{\partial x_j}\left(\alpha_\varepsilon \mu_{eff} \frac{\partial \varepsilon}{\partial x_j} \right) + \frac{C_{1\varepsilon}^*}{k} G_k - C_{2\varepsilon} \rho \frac{\varepsilon^2}{k} \tag{5}$$

With $\alpha_k = \alpha_\varepsilon$ =1.393 and $C_{2\varepsilon}$ =1.68. The production term in Equation (4) is given by:

$$G_k = \mu_t S^2 \tag{6}$$

and S is the modulus of the mean rate-of-strain tensor:

$$S \equiv \sqrt{2 S_{ij} S_{ij}} \quad , \quad S_{ij} = \frac{1}{2}\left(\frac{\partial \bar{u}_i}{\partial x_j} + \frac{\partial \bar{u}_j}{\partial x_i} \right)$$

Furthermore, the effective viscosity is calculated by:

$$\mu_t = \rho C_\mu \frac{k^2}{\varepsilon} \quad , \quad \mu_{eff} = \mu + \mu_t$$

with

C_μ=0.0845

and

$$C_{1\varepsilon}^* = C_{1\varepsilon} - \frac{\eta\left(1-\frac{\eta}{\eta_0}\right)}{1+\beta\eta^3} \quad , \quad \eta = \left(2S_{ij}.S_{ij}\right)^{1/2}\frac{k}{\varepsilon} \tag{7}$$

η_0=4.38, β=0.012, $C_{1\varepsilon}$=1.42

2. 2. Boundary Conditions A constant mixed velocity was specified at the inlet. The velocity was prescribed normal to the inflow boundary for each computation. Pressure outlet condition was chosen for the outlet of the domain. The impeller region was solved in a moving frame of reference, while the vanes and stator parts were solved in stationary reference frame. No-slip condition was assumed for all walls and the fluid was considered incompressible. The walls separating the rotary and stationary zones were defined as interior.

3. NUMERICAL MODEL AND MULTIPLE REFERENCE FRAME (MRF) TECHNIQUE

The pump impeller region is attached to a rotating frame and so it is solved in a rotating frame work via Multiple Reference Frame (MRF) technique. In this approach the rotational domain which consists of the impellers and the region surrounding them is simulated first. The resulting flow from the interface of the rotating and stationary frames is a boundary condition for simulating the stationary domain.

In this study, all simulations were performed using the commercial CFD software FLUENT 6.3. A pressure based finite volume method was used for this problem. Steady-state, incompressible, three-dimensional equations were solved. Turbulence was modeled using RNG k-ε model. The SIMPLEC algorithm was used for the pressure velocity coupling. The second order upwind difference scheme was used for the momentum, turbulence kinetic energy and dissipation rates equations. For each dependent variable, solution convergence was defined by monitoring the rates of change. The solution was considered converged when these rates decreased by three orders of magnitude.

4. GEOMETRY AND GRID

The whole hydraulic passage of the mixed-flow pump, which is the solution domain, is shown in Figure 1. According to the existing data from Mashhad power plant, which is the reference of this study, the pump was modeled by CFTurbo software, considering the techniques and information about the characteristics of the pump. Furthermore, to make the model perfect and preparing it by mesh generating for the solution domains, it was exported to Gambit software and it was well treated there. Having done all requirement of the model, it was finally simulated by FLUENT software and the results are presented in this paper. The whole domain is divided into 2 sub-domains. One sub-domain is the rotor domain which includes the impellers and the region between them. This zone is solved in a moving framework. The other sub-domain includes the vanes and the inlet and outlet regions which are solved in a stationary framework. This pump consists of 4 blades mixed flow impeller, and 9 stator vanes. The impeller diameter is 766 mm and the hub diameter is 167 mm.

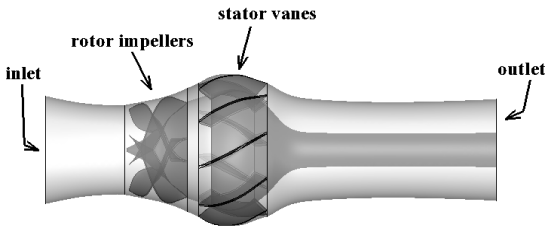

Figure 1. Pump impellers and stator vanes

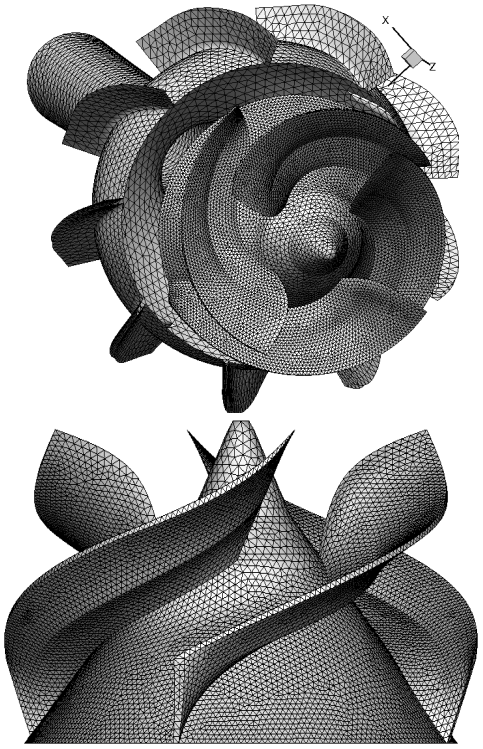

Figure 2. Mesh generated for the geometry

As shown in Figure2, complexity of the geometry yields using hybrid meshing scheme with tetrahedral cells in the solution domain. Relatively finer grids are used in critical regions like the impellers and surrounding moving domain where bubble formation and cavitation phenomenon may occur. In order to check the influence of the grids on the problem solution, mesh systems with different numbers of nodes were tested. Hence, grid independency is checked in this way. Table 1 shows grid sizes and computed quantities such as power and static pressure rise for the given cell arrangements

Here, mesh number of 718000 was assumed to be a reference point. It is observed that the results on different grids become closer to each other as the grid is refined. By continuing the refinement it can be seen that no remarkable approach to the reference data takes place according to the time and expenses that rises due to enhancing mesh numbers. Verifying variation percentages, mesh number of 718000 meshes was selected for this problem.

5. RESULT AND DISCUSSION

After choosing a proper mesh number and defining governing equations of the problem, the results are presented in this part. Figure 3 shows the performance curve of the pump for numerical simulation of the present study and experimental data obtained from the real pump. This figure is a good demonstration of the model behavior in comparison with the real pump in the power plant and its experimental performance curve. So this figure confirms our solution and in this way it can be said that the chosen model performed well and the results are reliable. The deviation exist in the curves due to the numerical assumptions and approximations utilized for the solution. Guide vanes usually aim at improving flow patterns and reducing hydraulic loss by converting some of the kinetic energy into pressure energy. As it is seen in Figure 4, the stator vanes made the most pressurized region by converting the kinetic energy, and at the outlet due to the pressure loss of the moving flow through the duct, the pressure diminishes slightly. On the other hand, the main part responsible for kinetic energy is pump impeller. So it can be concluded that the region surrounding the moving blades has the most velocity amount which admits the most kinetic energy that the pump offers to the fluid passing through it. Hence the lowest static pressure is observed in this region. Mainly, energy transfer from the pump to the fluid takes place in this domain.

Figure 5 shows the flow streamlines. In stator vanes the energy transform yields to flow circulation and the main reason is the low pressure regions existing in this domain.

TABLE 1. Grid independency for five grid systems

Grid points	Power [kW]	Variation (%)	Static pressure rise [m]	Variation (%)
82000	460.5	3	21.58	3.2
248000	468.5	1.5	21.97	1.4
543000	472.9	0.6	22.02	1.2
718000	475.9	0	22.3	0
930000	475.56	0.07	22.4	0.4

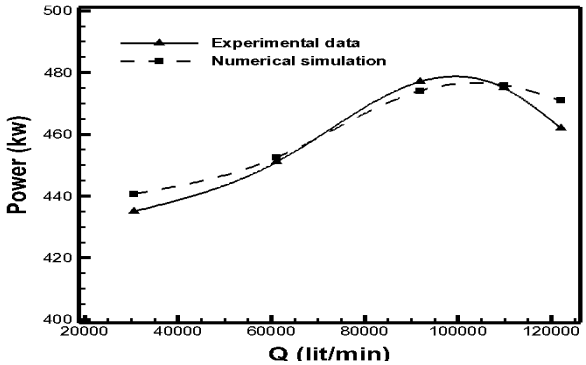

Figure 3. Comparison of numerical and experimental performance curves

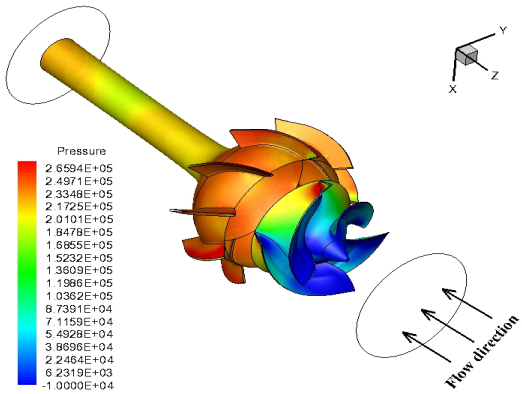

Figure 4. Pressure contour of the pump

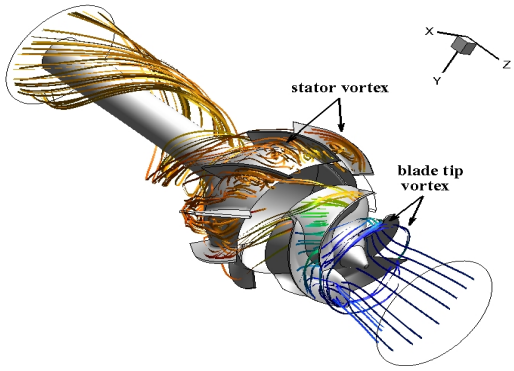

Figure 5. Streamlines of the whole domain

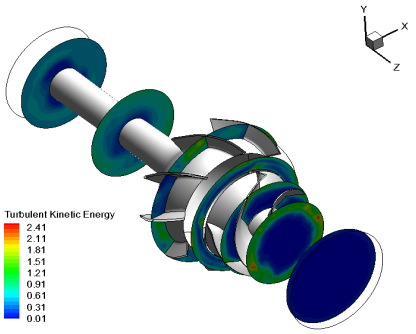

Figure 6. Turbulent kinetic energy (m^2/s^2) in different sections of the domain

Figure 6 is a demonstration of turbulent kinetic energy in different cross sections of the whole domain. This figure shows that the turbulent energy around the impellers region is higher than that in the impeller center as a result of the higher fluctuation of the flow velocity near the blades tips. Accordingly, the main objective of these vanes is to weaken the turbulent intensity and reduce the energy loss in the flow field. This effect of stator vanes is clearly seen in figure 6.

As it was mentioned previously, in this study the effect of pump speed on cavitation phenomenon was verified and the result is presented in Figure 7. In this figure six different cases are shown. From **a** to **f**, the speed changes by 500, 600, 743, 800, 900 and 1000 rpm, respectively where 743rpm is the nominal speed of the pump. Since the temperature is an important parameter in cavitation, for all cases the temperature is set to be 300K. This figure which is an iso-surface 3D contour shows the places where the pressure falls down to the critical pressure which yields to cavitation. It is seen that when the pump speed increases, due to great suction effect produced in the impeller, the critical pressure region spreads in the suction domain of the pump and after that moves slightly toward the downstream and so to the trailing edge of the blades. Also it is witnessed that this phenomenon didn't bound just to the surfaces of blades, and it grew in the fluid. It means that the bubble formation not only happens on blade surfaces, but also inside the flow. In low speeds of the pump, the leading edges of the blades are more probable to impose cavitation and the resulting corrosion. Another approach to show the cavitation phenomenon is pressure coefficient which is defined by:

$$C_p = \frac{p - p_{sat}}{\frac{1}{2}\rho_{ref} V_{ref}^{\ 2}}$$

where p_{sat} is the saturation pressure of the fluid for the temperature when phase change takes place. ρ_{ref} and V_{ref} are the density and velocity references of the fluid, respectively. According to the given definition, $C_p = 0$ shows the critical pressure coefficient for cavitation occurrence. As a result, in regions with negative pressure coefficient cavitaion exists. Figure 8 shows different states of pressure coefficient. Also it is obvious that due to the centrifugal movement of the fluid and so the bubbles, the bubble collapse which causes cavitatin corrosion take place in upper region of the place where the bubbles take form, and this is brightly shown in Figure 9.

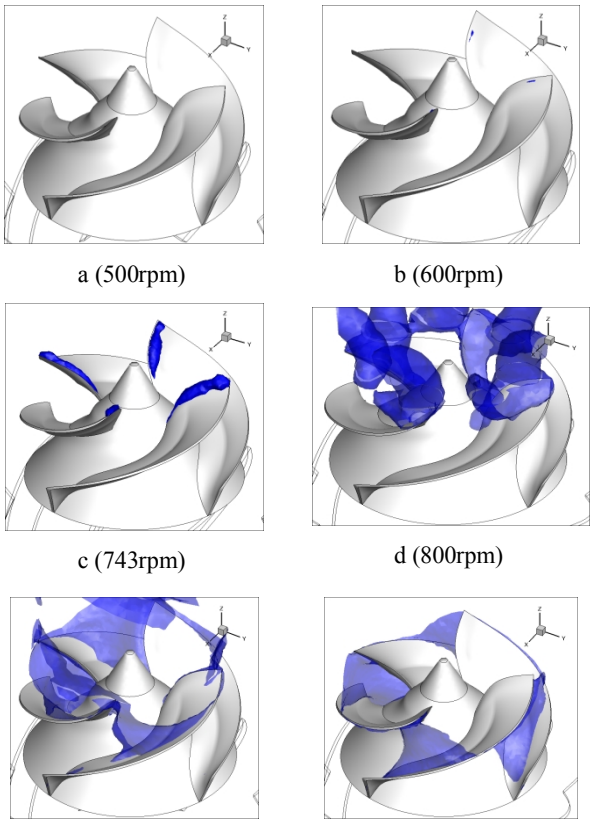

a (500rpm) b (600rpm)

c (743rpm) d (800rpm)

e (900rpm) f (1000rpm)

0Figure 7. Cavitation region for different pump speeds

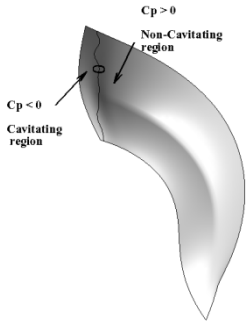

Figure 8. Pressure coefficient states on a blade

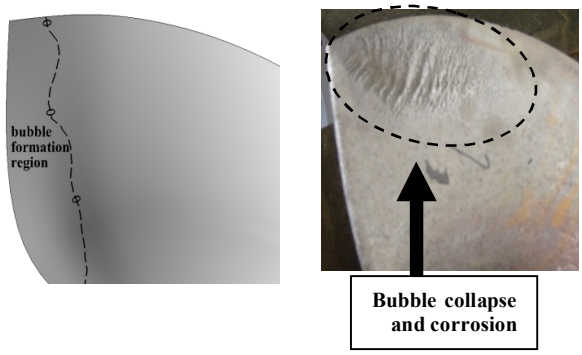

Figure 9. Demonstration of bubble formation region and its collapse

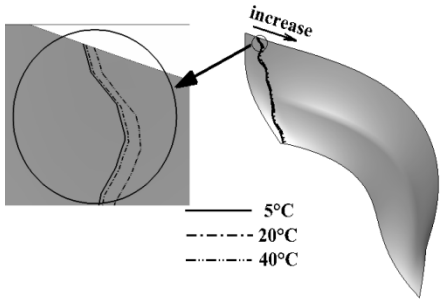

Figure 10. Temperature effect on cavitation

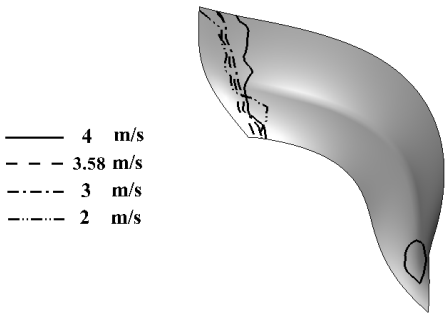

Figure 11. Flow rate effect on cavitation

As it was mentioned former, temperature is an effective parameter which deals with cavitation occurrence. In this problem different temperatures for a specific case (preferably the optimum operating condition) were investigated. The reason was the temperature change which happens due to different weather conditions in different seasons of a year. In this effort, the temperature variation from 5 to 40°C is analyzed. Figure 10 demonstrates a sample blade in which the critical pressure coefficient line is shown for three definite temperatures, 5, 20 and 40°C. According to this study when the temperature raises cavitation region slightly develops toward the trailing edge of the blade. However it is obvious that this parameter had a faint effect on cavitation enlargement due to limited temperature variations.

Another approach to the cavitation phenomenon verification was the effect of flow rate passing through the impellers on cavitation occurrence. When the flow rate is changed, the inlet velocity is changed accordingly. So in this literature for a fixed temperature (defined vaporization pressure) different inlet velocity values for the pump intake were assumed, namely 1, 2, 3, 3.58 and 4m/s. Simulation showed that for the case with lower inlet velocity e.g. value of 1m/s there was no sign of cavitation. This was because of static pressure enhancement which resulted from velocity reduction corresponding to Bernoulli's equation. When the flow rate is enhanced, due to the increase of velocity on blade surfaces the pressure falls down to the critical amount and this yields in cavitation occurrence. Figure 11 shows the subject. As it is obvious, for velocity of 4m/s larger region of the blade surface exposes to cavitation, and also the pressure at the trailing edge of the blade fell down to the critical pressure coefficient at this speed. There is no linear behavior for this phenomenon and attributed velocity, because it is seen that when the velocity amount vary from 2 to 3.58 there is no regular trend and the turbulent chaotic behavior of the fluid in this problem can be responsible for that. Finally, having witnessed the results, velocity of 3.58 which is the optimum velocity of the pump is the best amount for less cavitation corrosion

6. CONCLUSION

Numerical simulations of the three-dimensional steady turbulent flow in a mixed flow pump considering cavitation occurrence were successfully conducted using the commercial CFD software FLUENT 6.3. The results show the following:

(1) Moving reference frame approach and the mathematical model used in this study can be an acceptable candidate for simulation of the turbulent flow inside the mixed flow pump. The computational Q-H curve resulted from the simulation agreed well with reference (experimental) curves.

(2) Non-uniform velocity pattern distribution on leading edges of the blades and the tip vortexes in that region lead to higher turbulent energy in that region and this is obviously seen in Figures 5 & 6.

(3) The speed of the mixed flow pump has great effect on the place of cavitation occurrence and also its existence. Meanwhile low pump speed reduces the probability of cavitation happening, it reduces the operating efficiency noticeably. Consequently, an overall conclusion of cavitation preventing and operating efficiency can be helpful.

(4) Critical pressure coefficient can be a parameter which indicates cavitation onset. The vaporization pressure which governs bubble formation depends on the fluid temperature. Since the pump works in different temperatures, it was verified. But the results showed little effect of temperature on cavitation and it means that it is not a concerning parameter.

(5) The flow rate which is an important operational parameter for a pump has great influence on cavitation beginning and its development. This parameter is applied by changing the intake velocity of the pump. This literature shows that enhancing the flow rate diminishes the static pressure on blade surfaces and this yields to the enlargement of cavitaion region. But this cannot be a regular rule.

7. REFERENCES

1. Zhang, D.-s., Shi, W.-d., Bin, C. and Guan, X.-f., "Unsteady flow analysis and experimental investigation of axial-flow pump", ***Journal of Hydrodynamics, Ser. B***, Vol. 22, No. 1, (2010), 35-43.
2. Alpan, K. and Peng, W., "Suction reverse flow in an axial-flow pump", ***Journal of Fluids Engineering***, Vol. 113, No. 1, (1991), 90-97.
3. Zierke, W., Farrell, K. and Straka, W., "Measurements of the tip clearance flow for a high-reynolds-number axial-flow rotor", ***Transactions-American Society of Mechanical Engineers Journal of Turbomachinery***, Vol. 117, No., (1995), 522-522.
4. Zierke, W., Straka, W. and Taylor, P., "An experimental investigation of the flow through an axial-flow pump", ***Journal of Fluids Engineering***, Vol. 117, No. 3, (1995), 485-490.
5. Dupont, P., Caignaert, G., Bois, G. and Schneider, T., "Rotor-stator interactions in a vaned diffuser radial flow pump", in ASME Fluids Engineering Division Summer Meeting, American Society of Mechanical Engineers. (2005), 1087-1094.
6. Li, Y.-j. and Wang, F.-j., "Numerical investigation of performance of an axial-flow pump with inducer", ***Journal of Hydrodynamics, Ser. B***, Vol. 19, No. 6, (2007), 705-711.
7. Fu, j.W., Yao, j.L. and Guo, h.C., "Cfd simulation of 3d flow in large-bore axial-flow pump with half-elbow suction sump [j]", ***Journal of Hydrodynamics, Ser. B***, Vol. 18, No. 2, (2006), 243-247.
8. Fujun, W., Ling, Z. and Zhimin, Z., "Analysis on pressure fluctuation of unsteady flow in axial-flow pump", ***Journal of Hydraulic Engineering***, Vol. 38, No. 8, (2007), 1003-1009.
9. Shigmitsu, T., Furukawa, A. And Watanabe, S., "Internal flow measurement with ldv at design point of contra-rotating axial flow pump nihon kikai gakkai ronbunshu", ***Transactions of the Japan Society of Mechanical Engineers, Part B***, Vol. 74, No. 5, (2008), 1091-1097.
10. Watanabe, A., Yamashita, S. and Tsunenari, Y., "Flow measurement with ldv around rear rotor of contra-rotating axial flow pump at partial flow rate", ***Transactions of the Japan Society of Mechanical Engineers, Part B***, Vol. 74, No. 4, (2008), 850-855.
11. Gao, H., Lin, W. and Du, Z., "An investigation of the flow and overall performance in a water-jet axial flow pump based on computational fluid dynamics and inverse design method", ***Proceedings of the Institution of Mechanical Engineers, Part A: Journal of Power and Energy***, Vol. 222, No. 5, (2008), 517-527.
12. Chen, H.-X. And Zhu, B., "Analysis of numerical calculation on an axial-flow pump model with 0 installation angle ", ***Journal of Hydrodynamics (Ser. A)***, Vol. 4, (2009), 014.
13. Fan, H.-M., Hong, F.-W., Zhou, L.-D., Chen, Y.-S., Liang, Y. and LIU, Z.-m., "Design of implantable axial-flow blood pump and numerical studies on its performance", ***Journal of Hydrodynamics, Ser. B***, Vol. 21, No. 4, (2009), 445-452.
14. Huanming, H. and Hong, G., "Numerical simulation and experimental study on flow field in an axial flow pump", ***Journal of Shanghai Jiaotong University***, Vol. 43, No. 1, (2009), 124-128.
15. Shu, J.-J., "Modelling vaporous cavitation on fluid transients", ***International Journal of Pressure Vessels and Piping***, Vol. 80, No. 3, (2003), 187-195.
16. Čudina, M. and Prezelj, J., "Detection of cavitation in situ operation of kinetic pumps: Effect of cavitation on the characteristic discrete frequency component", ***Applied Acoustics***, Vol. 70, No. 9, (2009), 1175-1182.
17. Peng, Y.-C., Chen, X.-Y., Yan, C. and Hou, G.-X., "Numerical study of cavitation on the surface of the guide vane in three gorges hydropower unit", ***Journal of Hydrodynamics, Ser. B***, Vol. 22, No. 5, (2010), 703-708.
18. Escaler, X., Egusquiza, E., Farhat, M., Avellan, F. and Coussirat, M., "Detection of cavitation in hydraulic turbines", ***Mechanical Systems and Signal Processing***, Vol. 20, No. 4, (2006), 983-1007.
19. Jazi, A.M. and Rahimzadeh, H., "Detecting cavitation in globe valves by two methods: Characteristic diagrams and acoustic analysis", ***Applied Acoustics***, Vol. 70, No. 11, (2009), 1440-1445.
20. Mettin, R., Luther, S., Ohl, C.-D. and Lauterborn, W., "Acoustic cavitation structures and simulations by a particle model", ***Ultrasonics Sonochemistry***, Vol. 6, No. 1, (1999), 25-29.
21. Dular, M., Bachert, B., Stoffel, B. and Širok, B., "Relationship between cavitation structures and cavitation damage", ***Wear***, Vol. 257, No. 11, (2004), 1176-1184.
22. De, M.L., Shu, H.L. And Yu, L.W., "Les numerical simulation of cavitation bubble shedding on ale 25 and ale 15 hydrofoils ", ***Journal of Hydrodynamics***, Vol. 21, No. 6, (2009), 807-813.
23. Pouffary, B., Patella, R.F., Reboud, J.-L. and Lambert, P.-A., "Numerical simulation of 3d cavitating flows: Analysis of cavitation head drop in turbomachinery", ***Journal of Fluids Engineering***, Vol. 130, No. 6, (2008), 061301.
24. Ye, J.-M. And Xiong, Y., "Prediction of podded propeller cavitation using an unsteady surface panel method", ***Journal of Hydrodynamics, Ser. B***, Vol. 20, No. 6, (2008), 790-796.
25. Mirbagheri, S. and Mansouri, M., "Solution of flow field equations and verification of cavitations problem on spillway of the dam", ***International Journal of Engineering-Materials And Energy Research Center-***, Vol. 18, No. 1, (2005), 97.
26. Sadrnezhad, S., "Numerical solution for gate induced vibration due to under flow cavitation", ***International Journal of Engineering***, Vol. 14, No. 3, (2001), 183-194.
27. Gavzan, I.J. and Rad, M., "Influence of afterbody and boundary layer on cavitating flow", ***International Journal of Engineering-Transactions B: Applications***, Vol. 22, No. 2, (2009), 185-194.
28. Choudhury, D., "Introduction to the renormalization group method and turbulence modeling, Fluent Incorporated, (1993).

Numerical Simulation of Cavitation in Mixed Flow Pump

Y. Vazifeshenas , M. Farhadi, K. Sedighi , R. Shafaghat

Faculty of Mechanical Engineering, Babol University of Technology, Babol, Iran

P A P E R I N F O

Paper history:
Received 23 April 2014
Received in revised form 05 June 2015
Accepted 11 June 2015

Keywords:
Mixed-flow Pump
Multiple Reference Frame
Computational Fluid Dynamics
Cavitation

چکیده

هدف از این تحقیق ارزیابی عملکرد و رفتار سه بعدی جریان در یک پمپ جریان مختلط و چگونگی تاثیر پذیری پدیده کاویتاسیون از پارامترهای مختلف مانند دمای سیال، سرعت پمپ و نرخ جریان ورودی می باشد. از نرم افزار دینامیک سیالات محاسباتی فلوئنت برای شبیه سازی کل میدان جریان پمپ استفاده شده است. مدل توربولانسی RNG k-ε به همراه standard wall functions برای توجیه رفتار توربولانسی سیال بکار گرفته شده‌اند. پمپ مورد مطالعه چهار پره که بر توپی مخروطی سوار شده‌اند و بخش متحرک را تشکیل می دهند و نه پره ثابت در پائین دست که نقش پره های ثابت را بازی می کنند، دارد. بنابراین برهمکنش میان روتور–استاتور با تکنیک چند چارچوب مرجع (MRF) بحث شده است. نرخ جریان و سرعت پمپ پارامترهای کلیدی برای بررسی بوده‌اند. در حالیکه دبی ورودی پمپ و دور پمپ بطور گسترده بر پدیده کاویتاسیون تاثیر دارند، تغییرات دمایی که در فصول مختلف سال حاصل می شود تاثیر کمی بر کاویتاسیون داشته است. منطقه پیدایش کاویتاسیون که بر اساس فشار اشباع آن دمای خاص تعیین می شود برای حالت های مختلف روی یک پره نشان داده شده‌است.

***doi**: 10.5829/idosi.ije.2015.28.06c.17*